



1 **Shoreline and Land Use Land Cover Changes along the 2004 tsunami-**
2 **affected South Andaman Coast: Understanding Changing Hazard**
3 **Susceptibility**

4 Vikas Ghadamode^{1,2}, K. Kumari Aruna¹, Anand K Pandey^{1,2} Kirti Srivastava¹

5 1. CSIR- National Geophysical Research Institute, Hyderabad, 500007 India.
6 2. Academy of Scientific and Innovative Research (AcSIR), Ghaziabad 201002, India.

7

8 § Corresponding author: Email address: akpandey@ngri.res.in
9 Tel: +91-40-27012416

10

11 **Abstract**

12 The 2004-tsunami affected the South Andaman coast experiencing dynamic changes in the
13 coastal geomorphology making the region vulnerable. We focus on pre-and post-tsunami
14 shoreline and Land Use Land Cover changes for the period 2004, 2005, and 2022 to analyse
15 the dynamic change in hazard. We used GEBCO bathymetry data to calculate Run-up (m),
16 arrival times (Min), and inundation (m) at 13 different locations using the 2004 Sumatra
17 Earthquake source parameters. The Digital Shoreline Analysis System is used for the shoreline
18 change estimates. The Landsat data is used to calculate shoreline and LULC change in five
19 classes, namely Built-Up Areas, Forests, Inundation areas, Croplands, and water bodies during
20 the above period. We examine the correlation between the LULC changes and the dynamic
21 change in shoreline due to population flux, infrastructural growth, and Gross State Domestic
22 Product growth. India industry estimates the Andaman & Nicobar Islands losses exceed INR
23 10 billion during 2004 that would see a five-fold increase in economic loss due to a doubling
24 of built-up area, a three-fold increase in tourist inflow, and a population density growth. The
25 unsustainable decline in the forest cover, mangroves, and cropland would affect sustainability
26 during a disaster despite coastal safety measures.

27 **Keywords: Geomorphology, Land use Land cover, Shoreline, Tsunami, Remote sensing**

28



29 **1. Introduction:**

30 The Coastal shorelines are dynamic and highly vulnerable to erosion and accretion caused by
31 hydrodynamic, tectonic, geomorphic, and climate forcing including tsunamis, cyclones,
32 flooding, storm surges, wave action, wind and tide changes, and sea level variations (Nayak
33 2002; Boak & Turner 2005; Kumar et al. 2010; Mukhopadhyay et al. 2011). In addition to
34 natural coastal processes, coastal resources are constantly under stress due to anthropogenic
35 activities, such as industrialization, port construction, beach sand mining, garbage dumping,
36 urbanization, trade, tourism, and recreational activities, which significantly impact the
37 shoreline and results into damage to natural ecosystems (Yi et al. 2018; Davis, 2019). It is
38 important to regularly monitor spatio-temporal along shorelines, Land use / Land Cover
39 (LULC) and geomorphic features (Moran, 2003; Cooper et al. 2004; Scheffers et al. 2005;
40 Jayakumar & Malarvannan 2016). Several studies have been conducted to analyse various
41 coastal processes, including the mapping of shoreline change, LULC change detection and
42 analysis of geomorphological landforms using satellite data. The temporal multispectral
43 satellite data allow for the identification of regions undergoing erosion or accretion change
44 (Misra and Balaji, 2015; Kumari et al. 2012; Tonisso et al. 2012; Murali et al, 2013, Sudha
45 Rani et al, 2015; Rowland et al, 2022, Thieblemont et al, 2021). The Indian Ocean tsunami of
46 December 26, 2004 was triggered by a magnitude 9.3 undersea earthquake near the coast of
47 Sumatra, Indonesia and Caused massive destruction of the coastal ecosystem in the Andaman
48 region (Sheth et al. 2006; Ramalanjaona, 2011). Using remote sensing data and statistical
49 techniques the shoreline & geomorphology changes caused by the 2004 Sumatra tsunami
50 examined (Mouat and Lancaster 1996; Saraf and Choudhary, 1999; Reid et al. 2000; Chen
51 2002; Weng 2002; Siddiqui and Maajid 2004; Mujabar and Chandrasekhar 2011; Kumari et al.
52 2012; Tonisso et al. 2012; Jangir et al. 2014; Yuvaraj et al. 2014; Yunus and Narayana, 2015;
53 Yunus et al., 2016).

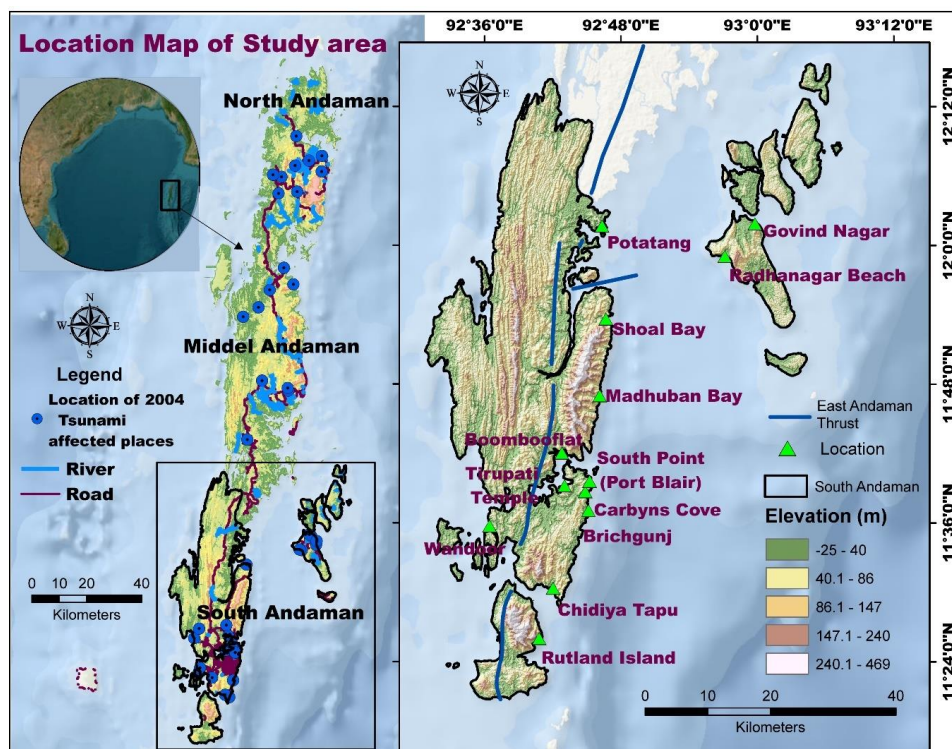
54 Since the 2004 Tsunami the Andaman and Nicobar Islands have experienced
55 remarkable population growth, infrastructural development, and flourishing tourism activities
56 progress over the past decade (Yuvaraj et al, 2014). The development is profound in the south
57 Andaman region. This is a cause of concern for the tsunami vulnerability as the region is prone
58 to very large earthquakes as it is a seismo-tectonically active plate boundary. In this study, we
59 Compute Tsunami arrival times, run-up heights, and inundation extent along the south
60 Andaman region. We also analyzed dynamic vulnerability using temporal and spatial changes
61 in shoreline and LULC for the tsunami-affected areas (Velmurugan et al, 2006; Ghadamode et



62 al, 2022). The analysis covers three time periods: 2004 (pre-tsunami), 2005 (post-tsunami), and
63 2022 (current status of shoreline and LULC) using multi-temporal Landsat data to map the
64 extent of shoreline changes in the EPR (End Point Rate) & NSM (NET Shoreline Movement)
65 Method. A relationship between LULC changes and vital socioeconomic factors such as
66 population dynamics, tourism trends, and the Gross State Domestic Product (GSDP) is
67 established to assess the potential future impacts of tsunamis in the region. The results would
68 provide actionable insights to the policymakers, coastal planners, and stakeholders in disaster
69 management and sustainable coastal development.

70 **2. Study Area**

71 South Andaman region with ~1,262 km² and a 413 km coastline is the southernmost island of
72 the Great Andaman where most of the Andaman Islands' population and infrastructure are
73 centrated. According to the 2011 Indian census, South Andaman has a population of 238,142
74 people, which increased to 266,900 in 2021 (estimate based on www.census2011.co.in). The
75 most habitable areas in the eastern part of South Andaman are located on low lands at bay
76 heads in addition to the higher slopes bordering bays and coastal flat lands (Ghosh et al. 2007).
77 The South Andaman region experienced devastation and losses during the 2004 Tsunami and
78 is vulnerable (Fig. 1). We selected 13 locations, namely South point in Port Blair, Rutland
79 Island, Corbyn's cove Beach, Madhuban Bay, Brichgunj, Chidiyatopu, Thirupatti Temple,
80 Wandoorjetty, Bamboo flat, Potatang, Shoal bay, Radha Nagar, and Govinda Nagar for
81 vulnerability assessment in the present study.



82
83

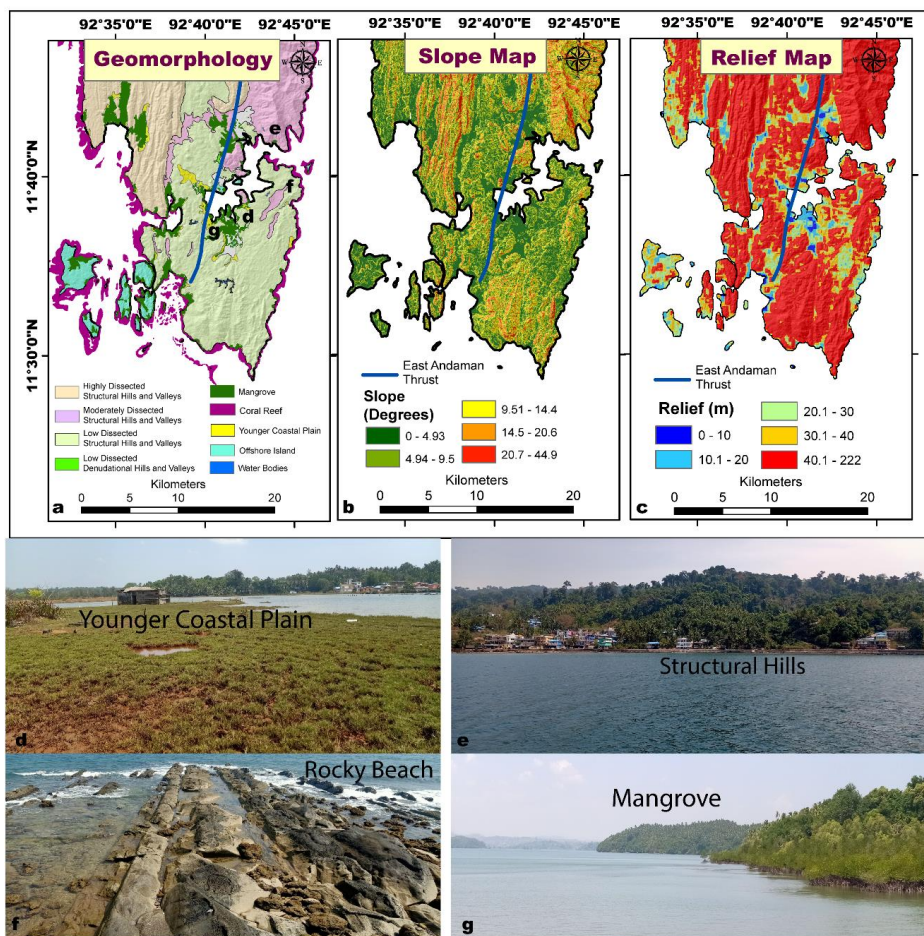
Figure 1 Location Map of the South Andaman Region (© Google Maps & © Google Earth).

84 The region's topography is primarily influenced by tectonic activity and weathering processes
85 (Curry, 2005; Bandopadhyay and Carter, 2017). The East Andaman Thrust also called East
86 Boundary Thrust is a linear/curvilinear ~500 km long fault zone and is the locus of ongoing
87 convergent and crustal deformation along the Sunda-Andaman plates. This structure is pivotal
88 in creating accretionary prisms within the outer-arc ridge of the Andaman and Nicobar
89 subduction zones (Fig. 1; Bhat et al., 2023).

90 The structure-bound major geomorphological features in South Andaman include hills, valleys,
91 beaches, mangroves, and coral reefs (Fig. 2a). The Younger coastal plain is a relatively flat and
92 low-lying area adjacent to the coastline, which is formed through the accumulation of
93 sediments brought by the ocean (2d). The highest peak on the island is Mount Harriet with
94 approximately 1,200 meters (3,937 feet) (southandaman.nic.in). The north-western part of
95 South Andaman is highly dissected whereas the North-eastern part is moderately dissected and
96 the Southern part is most likely low dissected structural hills and valleys (Fig. 2 a and e). The
97 island has a rough coastline with various bays, inlets, and headlands. A wave-cut platform is a
98 flat or gently sloping rock surface found along South Point coastlines in Port Blair (Fig. 2f). It
99 is formed through the erosive action of waves, which gradually wear away the rock over time.



100 These platforms can be exposed at low tide and are often a unique feature of rocky coastlines.
101 Coral reefs along the coast contribute to the formation of sandy beaches and barrier islands
102 (Reguero et al., 2018). Mangrove forests are found on coasts in South Andaman Island, primarily
103 in the brackish water and muddy sediments lagoons and tidal zone (Fig. 2g). Mangroves are
104 crucial in stabilizing coastal ecosystems and providing habitat for various species. Wandoor,
105 Chidya tapu, and Sippighat are some notable locations of mangrove forests in South Andaman
106 coastal areas. The upper slopes of the region are covered with high dissected structural hills
107 with dense pristine forest (Fig. 2a). The slope ranges between 0 to 44.9 degrees, with lower
108 slopes in the coastal region mostly inhibited and undergoing rapid coastline modification and
109 Land Use Change (Fig. 2 b and c). The North, Northeast, and Southern portions of South
110 Andaman have the steepest slope and relief area, while the Eastern, Southeastern, and western
111 parts have relatively lower slopes. The coastal plains in south Andaman are dynamic and prone
112 to tsunamis due to their location and active plate boundary, therefore studying shoreline change
113 and LULC change is especially important due to potential impacts on local communities and
114 ecosystems.



115
116 *Figure 2 (a) Geomorphology, (b) Slope map, (c) Relief Map, (d) the younger coastal plain, (e) Structural Hills, (f)*
117 *Rocky Beach with a wave-cut platform near south point, Port Blair, (g) Mangrove.*
118

119 3. Materials and Methods

120 To assess the vulnerability, it is imperative to generate a spatial dataset that may have a bearing
121 on assessing the dynamic changes.

122 3.1 Data Used

123 Landsat satellite data, such as Thematic Mapper (TM) and Operational Land Imagery
124 (OLI) sensor for the years 2004, 2005, and 2022 is used in the present study. The Shuttle Radar
125 Topography Mission (SRTM) Digital Elevation Model (DEM) is used to prepare the study
126 area's slope and relief map. This dataset analyzes shoreline and monitors the LULC changes
127 along the South Andaman coast. We used the General Bathymetry Chart of the Ocean
128 (GEBCO) for run-up and inundation studies along the south Andaman coastal areas (Table 1).

129



130 **Table 1:** Data used in the present study region

Data	Purpose	Month & Year	Resolution	Sources
GEBCO bathymetry	Inundation and Run-Up	2022	90 m	GEBCO
Landsat 5 TM and Landsat 8 OLI	LULC and Shoreline Change Analysis	March-2004 January-2005 March-2022	30 m	USGS Earth Explorer
SRTM DEM	Slope, Relief	-	30m	USGS Earth Explorer
Geomorphology	Geomorphology	-	1:250k	bhukosh.gsi.gov.in
Socioeconomic data	Population, Tourism, Gross State Domestic Product (GSDP)	1991-2021 2001-2020	-	(censusindia.gov.in) (Directorate of economics and statistics) (Rbi.org.in)

131

132 **3.2 Tsunami Run-ups and Inundation**

133 The 2004 earthquake rupture zone is divided into five segments by Ioualalen (2007) to
 134 simulate all stages of the tsunami. The earthquake source mechanism involves the rupture
 135 process, and magnitude is essential for tsunami hazard assessment. There have been several
 136 attempts to model tsunamis, calculate run-up heights, and evaluate their impact and hazards
 137 along coastal areas (Rani et al. 2011; Srivastava et al. 2021). For the propagation and run-up
 138 models, we used GEBCO bathymetry data with 81 arc seconds and 3 arc seconds resolution.
 139 The 26th December 2004 Sumatra earthquake ruptured about 1400km in length. Considering
 140 different slip distributions for the five segments (Table 2) TUNAMI-N2 code is used to
 141 compute the four grids A, B, C, & D. The exterior grid (A) in a very large domain as the tsunami
 142 propagates transoceanic and is interpolated into the B, C, and D grids. After giving the required
 143 inputs the program is compiled and executed to get the directivity map, wave amplitudes at
 144 different tide-gauge locations, and run-up heights.

145 **Table 2** Earthquake source parameters used to compute the deformation at the source along
 146 the Andaman-Sumatra Subduction Zone

Input Parameters	Seg1	Seg2	Seg3	Seg 4	Seg5
Longitude (DD)	94.57	93.90	93.21	92.60	92.87
Latitude (DD)	3.83	5.22	7.41	9.70	11.70
Focal Depth (km)	25	25	25	25	25
Strike angle (°)	323	348	338	356	10
Rake (°)	90	90	90	90	90
Slip (m)	18	23	12	12	12



Fault Length (km)	220	150	390	150	350
Fault Width (km)	130	130	125	95	95
Dip (°)	12	12	12	12	12

147

148 **3.3 Shoreline Analysis in DSAS**

149 To estimate shoreline changes, the USGS's digital shoreline analysis system (DSAS) version
150 5.1 (an extension of ArcGIS) is used. The procedures are executed in 4 steps: shoreline
151 digitization, baseline generation, transect generation, and computation of the rate of shoreline
152 change (Nithu Raj et al. 2020; Natarajan et al., 2021). The digitized shorelines for
153 2004, 2005 and 2022 years are added to a personal geodatabase in a single shapefile. The
154 shoreline image data is added to the attributes as MM/DD/YYYY, and the baseline is in the
155 meter UTM projected coordinate system. To estimate rates of change, DSAS uses baseline
156 measurements of a time series of shorelines and a shapefile (Leatherman and Clow, 1983). The
157 process of generating transects involves initially choosing a predefined set of parameters from
158 the personal geodatabase, including settings for the baseline and shoreline. Subsequently, we
159 placed these transects perpendicular to the shoreline, extending 800 meters at intervals of 150
160 meters along the entire shoreline, originating from the baseline. To ensure a smoother outcome,
161 a 50-meter smoothing distance was applied using the 'cast transects' tool within DSAS. In this
162 study, we employ statistical methodologies such as the End Point Rate (EPR) and Net Shoreline
163 Movement (NSM) to analyze the data.

164 **3.3.1 Net Shoreline Movement (NSM)**

165 NSM is a statistical parameter used to determine the net change in the shoreline position over
166 a specific period. It is calculated by finding the actual distance between the most recent
167 shoreline (in this case, 2022) and the oldest shoreline (2004) along each transect placed
168 perpendicular to the shorelines. The formula for NSM can be expressed as:

$$169 \quad \text{NSM} = \{d_{2022} - d_{2004}\}m$$

170 **3.3.2 End Point Rate (EPR)**

171 EPR is a statistical parameter used to quantify the rate of shoreline change over time. It is
172 calculated by dividing the Net Shoreline Movement (NSM) by the time elapsed between the
173 oldest and most recent shoreline measurements. The formula for EPR can be expressed as This
174 calculation provides a measure of how much the shoreline has shifted per year, indicating the
175 rate of erosion or accretion. It is important to have data from at least two shoreline dates (Dolan
176 et al. 1991; Crowell et al. 1997).



177
$$EPR = \left\{ \frac{d_{2022} - d_{2004}}{t_{2022} - t_{2004}} \right\}$$

178 **3.4 Land Use Land Cover Analysis (LULC)**

179 The LULC map uses Landsat 5 TM (2004 and 2005) and Landsat 8 OLI (2022). False Colour
180 Composite (FCC) satellite images combine near-infrared, red, and green bands to delineate five
181 different classes Forest, built-up, Cropland, Water bodies, and Inundated area. (Prabhbir and
182 Kamlesh, 2011). Tone, texture, size, shape, pattern, association, and other visual interpretation
183 techniques also were used to interpret different land use classes. Maximum likelihood is a
184 supervised classification method used in this study to detect LULC change. Each pixel in the
185 classified Landsat images varies over time due to changes in land cover.

186 **4. Results**

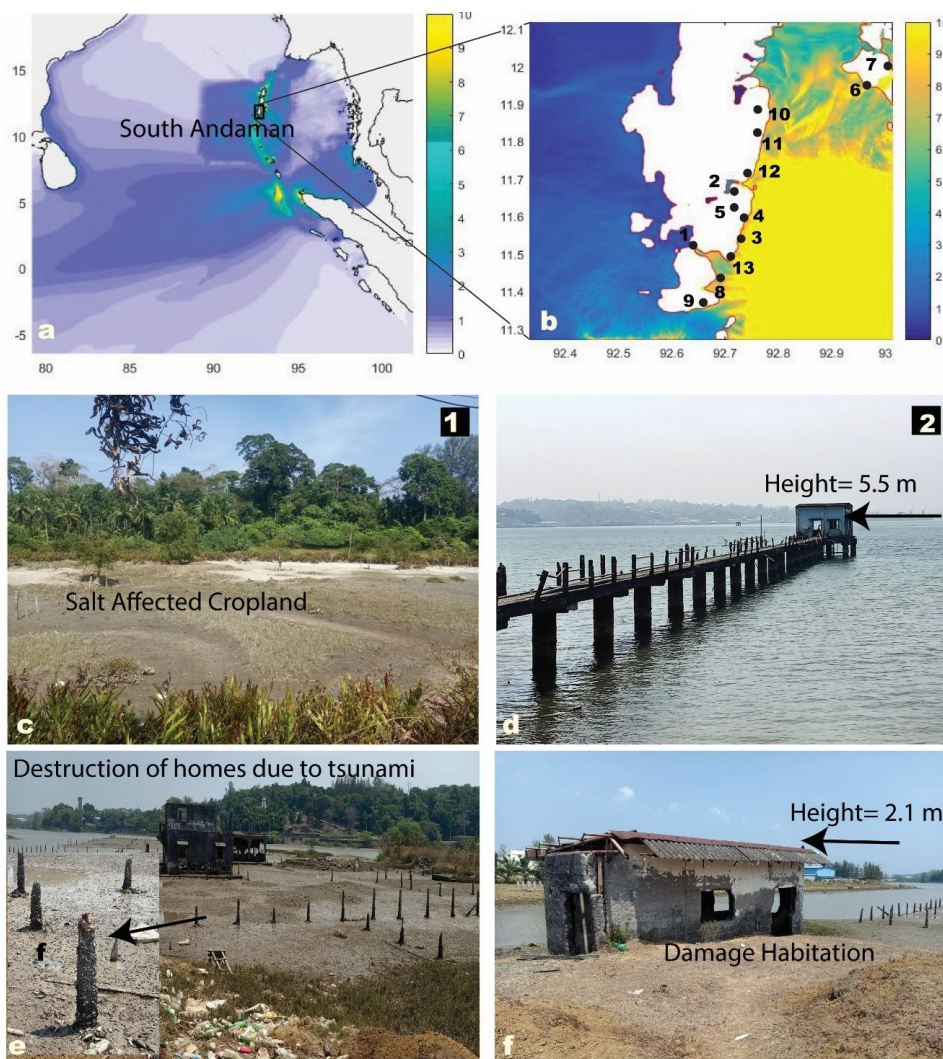
187 An analysis of the 2004 tsunamigenic earthquake's impact on the South Andaman region,
188 focusing on tsunami directivity, arrival times, run-up heights, shoreline changes, and LULC
189 impact is examined in detail

190 **4.1 Tsunami studies along the South Andaman Region**

191 The 2004 tsunamigenic earthquake is modeled to quantify the tsunami propagation, arrival
192 times, and run-ups at different locations along the South Andaman region. The initial deformation
193 at the source is computed for the fault parameters (Table 2). The Directivity map shows that most
194 of the energy propagation is in the East-West Direction (Fig. 3). The arrival times (Minutes), run-
195 up height (meter), and Inundation extent (meter) at 13 different locations along the South Andaman
196 region (Table 3) is considered for further analysis. The results show that the run-up heights range
197 from 1 to 13 m, arrival times range from 27 to 58 min, and the inundation extent range from 90 to
198 950 m. This suggests a significant variability in the impact of the tsunami across the South
199 Andaman Region. Shoal Bay recorded the highest inundation extent of 950 meters and experienced
200 the highest run-up height of 13 meters, indicating significant wave impact (Fig. 3b; Table 3).
201 Corbyns Cove Beach and Rutland Island experienced significant inundation distances, exceeding
202 700 meters (Fig.3b, Table 3). Potatang, Corbyns Cove Beach, and Brichgunj also recorded
203 relatively high run-up heights that exceeded 9 meters (Table 3). The tsunami arrived at Thirupatti
204 Temple after 38 minutes, suggesting a delayed impact compared to other locations. Most locations
205 experienced arrival times between 27 and 58 minutes, indicating a relatively quick propagation of
206 the tsunami wave. At some locations, however, the tsunami arrived early. Jain et al. (2005) have
207 mentioned that tsunami waves arrived between 40 to 50 minutes in the Andaman and Nicobar



208 Islands. Our results also agree with Cho et al. (2008) and Prerna et al. (2015) who computed the
209 tsunami runup heights at a few of the locations considered in the present study.



210

211 *Figure 3 (a) Directivity of the tsunami Wave Propagation of December 2004 Sumatra tsunami (b) Run-ups at*
212 *different locations along the south Andaman Coast (c) showing Stagnation of Tsunami water in the agricultural*
213 *land and Low laying Area in Port Blair, (d) Fully damaged construction bridge in Bombooflat. (c, d) shows damage*
214 *to the house near the Sippighat area (Photo: 01/03/2023).*

215

216

217

218



219 **Table 3** Estimated Run-up heights, Arrival Times, and inundations at the study region from
 220 the Sumatra tsunami

SN	Locations	Longitude (DD)	Latitude (DD)	Arrival Time (Mins)	Runup (m)	Inundation (m)
1	Wandoorjetty	92.614750	11.581667	36.5	3.5	450
2	Bombooflat	92.715417	11.700722	42	5.5	90
3	Corbyns Cove Beach	92.770916	11.642372	33	12.7	900
4	South Point, Port Blair	92.702917	11.652389	31.5	9.6	550
5	Thirupatti Temple	92.703861	11.581694	38	1	200
6	Radha Nagar	92.951722	11.979306	54	2.6	156
7	Govinda Nagar	92.989139	12.030167	58	3.6	195
8	Chidiyatopu	92.716639	11.499306	36	3.9	585
9	Rutland Island	92.703818	11.431497	27	6	700
10	Shoal Bay	92.795963	11.934202	56	13	950
11	Potatang	92.801282	12.027380	58	12.5	210
12	Madhuban Bay	92.785534	11.782775	54	6.9	210
13	Brichgunj	92.770162	11.618980	30	10	585

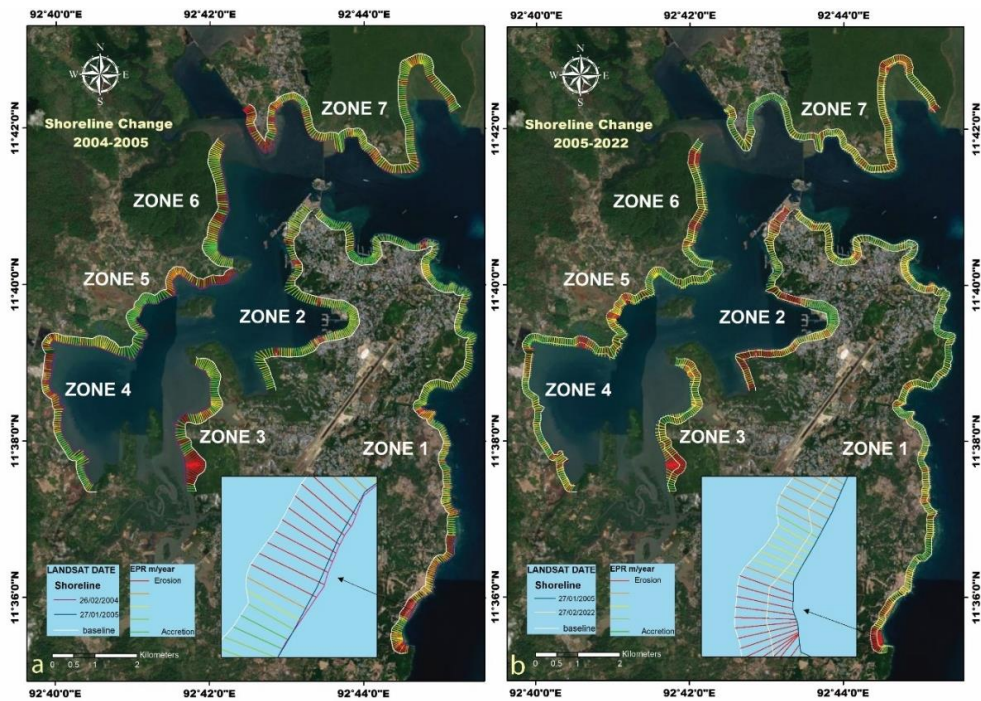
221

222 **4.2 Shoreline Change during Tsunami (2004-2005) and post-tsunami (2005-2021)**

223 The south Andaman coasts are divided into seven zones based on proximity with the
 224 inundation studies to calculate Net shoreline movement (NSM), and End Point Rate (EPR) to
 225 understand the short-term and long-term changes impact of coastal erosion (Fig. 4, Supplement
 226 Fig. S1-S7). The NSM and EPR rates are calculated over two separate time frames to
 227 comprehend the damages caused by tsunamigenic and regular wind-wave-surge events in
 228 South Andaman Island. These zones were used to understand erosion and accretion rates
 229 between (i) 2004 - 2005 (Fig. 4a), and (ii) 2005-2022 (Fig. 4b). The EPR and NSM values from
 230 2004 to 2005 indicate the direct effect of tsunami waves, whereas 2005 to 2022 values represent
 231 periodic wind-wave-surge dynamics. Periodic coastal shoreline changes refer to the regular and
 232 repeating fluctuations in the position of the shoreline along the coast. These changes can be
 233 influenced by natural and human-induced factors. A total of 1,083 transects are created at 50-
 234 meter intervals, distributed among the zones as follows: Zone 1 (339 transects), Zone 2 (147
 235 transects), Zone 3 (89 transects), Zone 4 (74 transects), Zone 5 (137 transects), Zone 6 (73



236 transects), and Zone 7 (220 transects). The shoreline variation rates indicate both positive
237 accretion and negative erosion (Fig. 5, Table 4). The EPR rate Changes in meters per year
238 (m/y) for the periods 2004-2005 show a higher erosion rate compared to 2005-2022,
239 particularly in Zones 3, 4, and 5 (Fig. 5a). The NSM rates, focused on two distinct time frames,
240 indicate the NSM rates during the tsunami, for the year of 2004-2005 (Fig. 5b), and the NSM
241 rates over the extended 17-year period from 2005 to 2022 are measured in meters (Fig. 5c).
242 The detailed analysis of the maximum (accretion), minimum (erosion), and mean shoreline
243 changes for each of the seven zones that occurred during the tsunami event and the post-
244 tsunami period are discussed below.



245
246 Figure 4: Shoreline changes observed (a) during 2004-05 due to the tsunamigenic process and (b) from 2005-
247 2022 due to wind wave surges overlaid on Google Earth images (© Google Earth). The affected coastline is
248 subdivided into seven distinct zones for detailed analysis.



249

250 *Figure 5: (a) The rates of erosion and accretion in seven distinct areas along the South Andaman shoreline using*
 251 *EPR methods, and (b, c) NSM have been conducted between the years 2004-2005 and 2005-2022. Highlighted*
 252 *color indicating high erosion zone*

253

254 **Table 4** Shoreline change in southern Andaman is observed for 2004-2005 and 2005-2022
 255 using USGS's DSAS methods.

ZONE		2004-2005		2005-2022	
		EPR(m/y)	NSM(m)	EPR(m/y)	NSM (m)
ZONE 1	Mean	-2.85	-2.62	-2.55	-43.57
	Minimum	-23.9	-21.29	-9.44	-161.21
	Maximum	12.05	11.06	0	0
ZONE 2	Mean	-0.54	-0.50	-1.0639	-18.174
	Minimum	-7.17	-6.58	-4.56	-77.93
	Maximum	6.54	6	3.25	55.56
ZONE 3	Mean	-9.92	-8.11	-7.10	-121.51
	Minimum	-24.71	-23.27	-19.87	-339.51
	Maximum	5.58	4.37	-1.02	-17.42
ZONE 4	Mean	-7.92	-7.72	-2.24	-38.34
	Minimum	-24.47	-22.46	-11.42	-195.03



	Maximum	6.23	5.72	-0.79	-13.42
ZONE 5	Mean	-6.594	-6.05	-2.94	-50.26
	Minimum	-21.47	-19.7	-7.95	-135.83
	Maximum	10.88	9.99	-1.03	-17.54
ZONE 6	Mean	-9.74	-8.94	-4.92	-84.05
	Minimum	-21.18	-19.44	-7.75	-132.39
	Maximum	-1.46	-1.34	-1.86	-31.73
ZONE 7	Mean	-2.16	-1.986	-2.43	-41.56
	Minimum	-18.65	-17.29	-11.7	-199.96
	Maximum	9.77	8.97	-0.04	-0.61

256

257 ZONE 1: This zone experienced a combination of erosion and accretion between 2004-05 and
 258 2005-21. The maximum erosion rates are observed at Megapoda, with an EPR of -23.9
 259 m/y. and -9.44 m/y., NSM analysis shows the estimated erosion is -21.29m and -161.21m
 260 respectively (Fig. SM 1 a, b, Table 6). The southern part of South Andaman Island has
 261 more shoreline erosion rather than accretion, which can be attributed to the heightened
 262 impact of tsunamis on the southern region, a phenomenon that is more significant when
 263 compared to the northern part of South Andaman Island. These Sediments eroded from
 264 one coastline area are often transported along the shoreline by the longshore currents.
 265 The angle of wave approach creates these currents and is responsible for moving
 266 sediment parallel to the coastline.

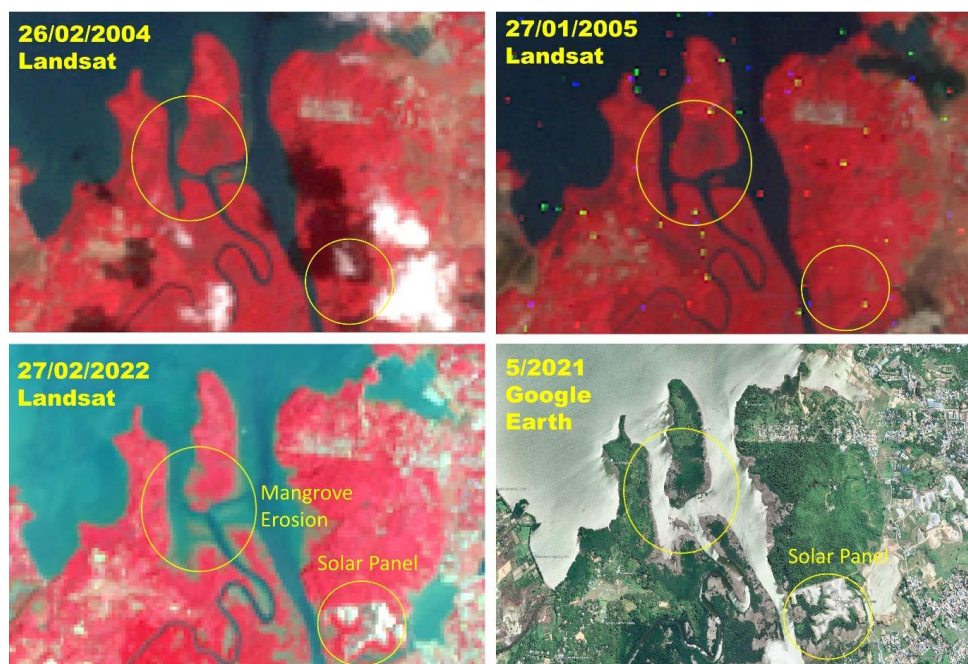
267 ZONE 2: This zone experienced a combination of erosion and accretion between 2004-05 and
 268 2005-21. The maximum rate of erosion is -7.17 m/y and -4.56 m/y (EPR) was recorded
 269 at IOC Colony, while the maximum accretion rate of 6.54 m/y and 3.25 m/y (EPR) was
 270 observed at Ashwin Nagar Respectively. The NSM analysis indicated a shoreline retreat
 271 of -6.58 m at IOC Colony and -77.93 m advancement at Ashwin Nagar. The jetties in the
 272 Jungli Ghat port played a role in controlling erosion and accretion at these sites (Fig. SM-
 273 2, Table 6).

274 ZONE 3: This zone experienced a combination of erosion and accretion between 2004-05 and
 275 2005-21. The maximum erosion rate is -24.71 m/y and -19.87 (EPR) at Flat Bay, while
 276 the maximum accretion rate is 5.58 m/y and (EPR) at NLC Limited. The NSM analysis
 277 revealed a shoreline retreat of -23.27 m and -339.51 m at Flat Bay. High wave energy
 278 and exposure to strong currents, which are more common near Flat Bay, can lead to
 279 increased erosion of mangrove shorelines (Fig. SM 3, Table 6).

280 ZONE 4: This zone experienced a combination of erosion and accretion between 2004-05 and
 281 2005-21. The maximum erosion rate is -24.47 m/y at Ferrargunj and -11.24 m/y (EPR)
 282 at PLK Creek Resort, NSM estimated erosion is -22.46 m and -195.03m at Chouldari



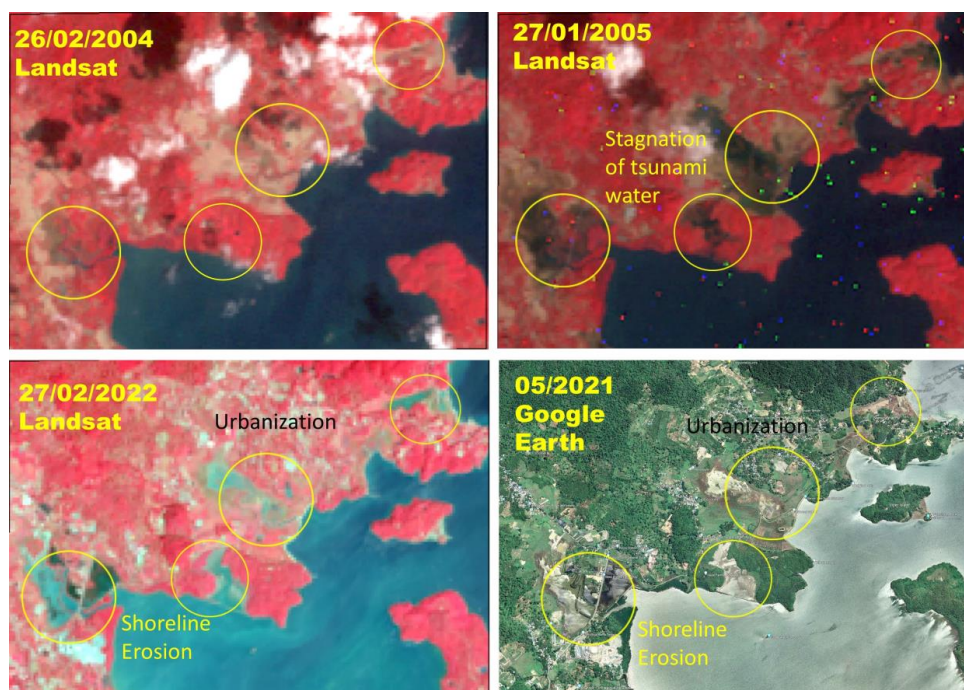
283 (Fig. SM 4). We observed the shoreline erosion area using the Landsat time-lapse satellite
284 images between 2004-2005, and 2022 near Flat Bay, South Andaman, has revealed
285 noteworthy environmental changes. The dark blue color observed in 2004 and 2005
286 indicates the presence of deep-water bodies, whereas the light blue color in the 2022
287 image suggests the water bodies have become shallow with significant fresh sediment
288 load.
289



290
291 *Figure 6 shows a time-lapse satellite imagery of Landsat 8 FCC near the Flat Bay area (marked in yellow circle)*
292 *during the years 2004 and 2005 showing robust mangrove coverage is evident. However, when comparing the*
293 *Landsat 8 image in 2022 and the corresponding Google Earth image (© Google Earth), it is apparent that the*
294 *mangrove ecosystem in this area has experienced substantial erosion and the development of Solar panels.*

295
296 **ZONE 5:** The maximum erosion rate of -21.47 m/y (2004-05) and -7.95 (EPR 2005-22) is
297 recorded at Mithakhari. According to the NSM analysis, the shoreline retreated by -19.7
298 m and -132.39 meters at Mithakhari (Fig. SM 5). In this zone, Coastal development,
299 infrastructure construction, and alteration of natural hydrological patterns can disrupt
300 sediment transport and exacerbate erosion.

301



302

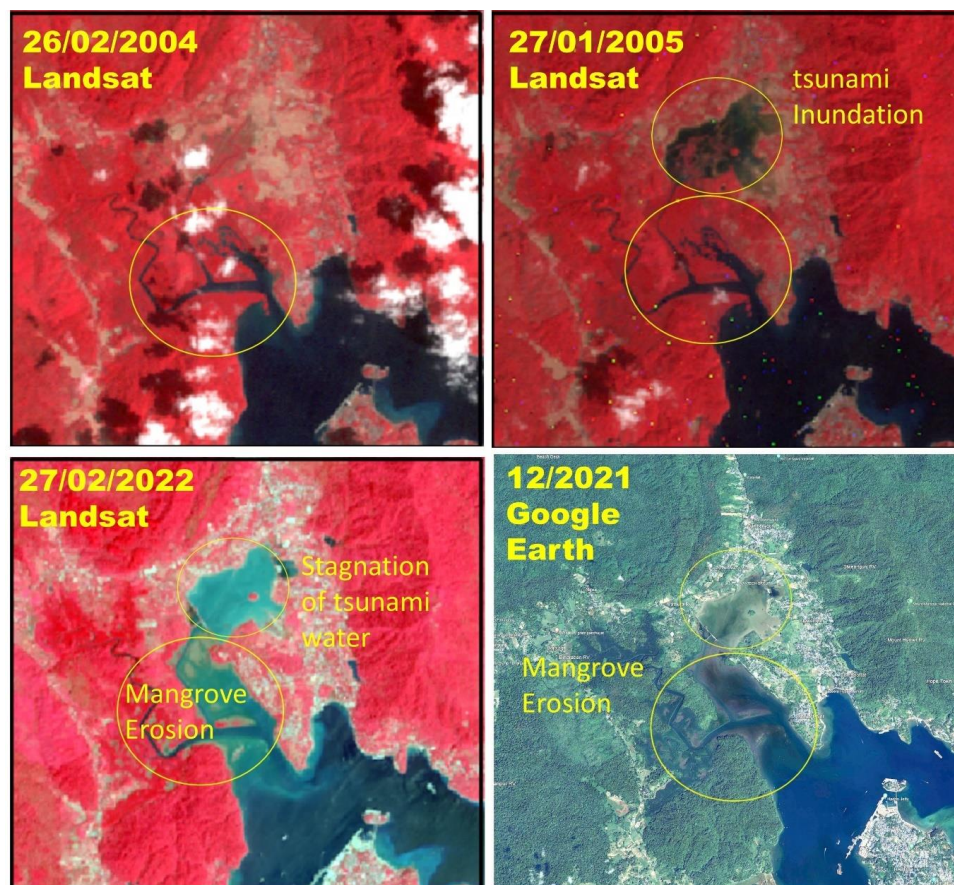
303 *Figure 7 shows Landsat 8 time-lapse imagery and © Google Earth imagery near the Ograbraj and Mithakhari*
304 *region depicting the erosion activity during and after the tsunami and the imagery shows significant growth in*
305 *the built-up areas surrounding the tsunami-affected areas in 2004.*

306

307 **ZONE 6:** This zone is predominantly affected by erosion, with no observed accretion. The
308 maximum erosion rate is -21.18 m/y and -7.75 m/y (EPR) at Namunaghar, and the NSM
309 estimated erosion is -19.44 m and -132.39m at Namunaghar (Fig. SM 6). In February
310 2004, immediately before the catastrophic tsunami event, there was no observable
311 presence of stagnant water in the area (Fig. 8). However, by January 2005, following the
312 tsunami, the images distinctly exhibited the stagnant water. In February 2022, the same
313 location exhibited substantial shoreline erosion within the extensive mangrove and
314 agricultural area, accompanied by increased urban development along the shoreline. The
315 urban development progression is also validated using Google satellite imagery. The
316 sediment carried by ocean currents deposited in low-lying areas revealed caused
317 shallowing and significant changes in ocean water color.

318

319



320

321 *Figure 8 shows the Change detection of the shoreline using Landsat 8 time-lapse imagery and © Google Earth*
322 *imagery for 2004 before, 2005 after the tsunami, and the 2022 present status of the shoreline.*

323

324 **ZONE 7:** This zone experienced a combination of erosion and accretion between 2004-05 and
325 2005-21. The maximum erosion rate is -8.36 m/y and -11.7 m/y (EPR) at Shore Point,
326 while the maximum accretion rate is 9.77 m/y (EPR). The NSM analysis indicated an
327 erosion of -17.29 m at Shore Point and -199.96 meters at North Bay (Fig. SM 7). Notably,
328 a tsunami with a height of 9.6 meters is observed at Shore Point.

329 The natural rate of shoreline movement in the South Andaman region has increased
330 following the tsunami event, which is attributed to several factors, including the removal of
331 vegetation cover, the softening of exposed bedrock, and the destabilization of unconsolidated
332 materials caused by the tsunami, all of which have made the region more susceptible to erosion



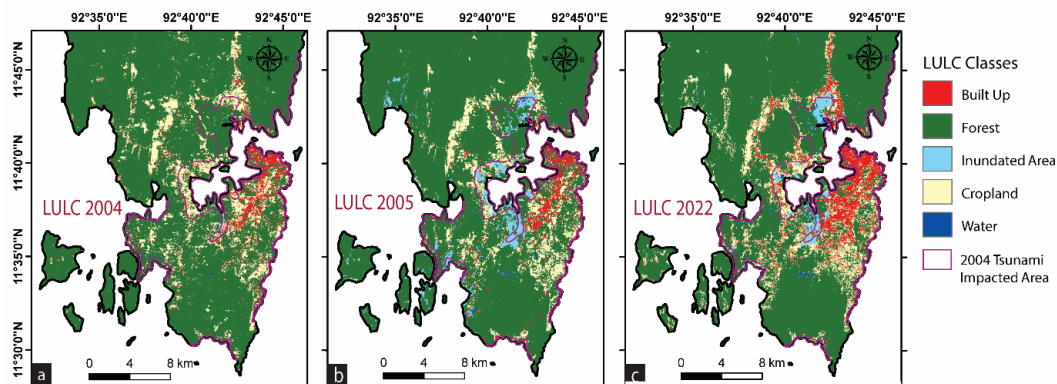
333 (Yunus et al., 2016). Comparing the erosion and accretion rates between the 2004-05 and 2005
334 -2022 periods, it is observed that the erosion rates were significantly less in the latter years.

335

336 4.3 Land Use and Land Cover (LULC) Analysis

337 The LULC is categorized into 5 distinct classes Built-up, Forest, Inundation, Cropland, and
338 water Bodies (Fig. 9). The overall accuracy obtained is 80%, 83%, and 82% with a quantitative
339 assessment of K_{hat} (Kappa) coefficient is 0.741, 0.762 and 0.759 for 2004,2005 and 2022
340 images, respectively. Our primary objective is to determine the extent of land use pattern
341 changes from 2004 to 2022 in areas affected by the 2004 tsunami. Several researchers have
342 already examined the vulnerability and impact of the 2004 tsunami on South Andaman
343 including (Velmurugan et al. 2006; Debjani et al. 2012; Sachithanandam,2014).

344 The LULC classification for the South Andaman region in tsunami-impacted areas in
345 the years 2004, 2005, and 2022 reveals significant changes (Fig. 9, Table 5): 1) The built-up
346 area decreased from ~7.38% in 2004 to 6.23% in 2005, marking a 1.15% decrease. However,
347 it subsequently increased by 11.11% by 2022. 2) Cropland coverage decreased from around
348 22.12% in 2004 to ~11.93% in 2005, indicating a substantial reduction of 10.19%. It then
349 increased to 17.15% by 2022. 3) Inundation areas increased from about 3.29% in 2004 to
350 27.65% in 2005, showing a notable rise of 24.36%. However, by 2022, they decreased by
351 ~18.57%. 4) Forested areas saw a significant decrease from ~66.46% in 2004 to about 51.10%
352 in 2005, signifying a reduction of 15.36%. This decrease persisted in 2022, remaining at
353 ~51.10%. 5) Water bodies covered around 0.62% of the area in 2004, which increased slightly
354 to about 0.76% in 2005. By 2022, there is a more significant increase, reaching 2.05%.



355

356 Figure 9 (a) LULC 2004 (b) LULC 2005, and (c) LULC 2022 in tsunami-impacted areas (pink color) and South
357 Andaman.



358

359 **Table 5** LULC Analysis for 2004, 2005 to 2022 in tsunami impacted area

LULC	2004 Area in km ²	2004 % of Area	2005 Area in km ²	2005 % of Area	2022 Area in km ²	2022 % of Area
Built-Up	3.57	7.38	3.01	6.23	5.38	11.11
Forest	32.19	66.46	25.79	53.40	24.74	51.10
Inundation Area	1.64	3.39	13.36	27.65	8.99	18.57
Cropland	10.71	22.12	5.76	11.93	24.74	17.15
Water Bodies	0.30	0.62	0.36	0.76	0.99	2.05
Total Area (Sq. Km)	48	100	48	100	48	100

360

361 The LULC classification for the South Andaman region in the years 2004, 2005, and 2022
362 shows significant changes (Figure 9, Table 6)

363 **1) Built-Up Area:** In 2004, the built-up area covered 19.92 km², constituting ~3.84% of the
364 total study area. By 2005, this area reduced to 17.66 km², accounting for 3.41% of the
365 total area. by 2022, there was a significant expansion, with the built-up area occupying
366 45.07 km², representing 8.68% of the total region.

367 **2) Forest:** In 2004, forests dominated the landscape, covering 432.85 km², which was
368 approximately 83.43% of the total study area. By 2005, this forested area slightly
369 decreased to 420.79 km², comprising 81.27% of the total area. However, by 2022, the
370 forest cover continued to decline, with an area of 408.66 km², accounting for 78.78% of
371 the total region.

372 **3) Inundation Area:** In 2004, the inundation area was limited, covering 3.40 km² or 0.65% of
373 the total area. In 2005, there was a substantial increase, expanding to 28.41 km², which
374 represented 5.48% of the total area. By 2022, the inundation area decreased to 13.89 km²,
375 making up 2.66% of the total region.

376 **4) Cropland:** Cropland covered 61.77 km² in 2004, accounting for 11.90% of the total study
377 area. By 2005, this area reduced to 49.34 km², representing 9.53% of the total area. In
378 2022, the cropland area further decreased to 48.65 km², making up 9.37% of the total
379 region.

380 **5) Water Bodies:** In 2004, water bodies covered a small area of 0.83 km², which was
381 approximately 0.16% of the total area. By 2005, this area slightly increased to 1.54 km²,
382 constituting 0.29% of the total region. In 2022, there was a more significant expansion,
383 with water bodies occupying 2.45 km², accounting for 0.47% of the total area.



384 **Table 6** LULC Analysis for 2004, 2005 to 2022 in the Study region

LULC	2004 Area in km ²	2004 % of Area	2005 Area in km ²	2005 % of Area	2022 Area in km ²	2022 % of Area
Built-Up	19.92	3.84	17.66	3.41	45.07	8.68
Forest	432.85	83.43	420.79	81.27	408.66	78.78
Inundation Area	3.40	0.65	28.41	5.48	13.89	2.66
Cropland	61.77	11.90	49.34	9.53	48.65	9.37
Water Bodies	0.83	0.16	1.54	0.29	2.45	0.47
Total Area (Sq. Km)	518	100	518	100	518	100

385

386 **5. Discussion**

387 The complex interaction between geomorphology, shoreline change, LULC changes, and
388 economic factors in tsunami vulnerability and impact assessment in South Andaman is
389 discussed below;

390 **5.1 Shoreline changes VS LULC**

391 The impact of tsunamis varies due to differences in landforms, relief, slope, elevation, and the
392 presence (or absence) of natural barriers such as coral reefs and mangroves. It has been
393 observed that for a given water depth on the shelf, if the continental slope is steeper, greater
394 mangrove cover, greater relief, and higher elevation can result in a greater amount of energy
395 being reflected back, leading to a smaller tsunami wave height on the shelf. On the other hand,
396 with a flatter slope, low relief, and less vegetation cover area on the coastal side, the reduced
397 reflection and effect of shoaling can increase tsunami wave height (Siva et al. 2016). Coastal
398 erosion is a natural process in south Andaman that occurs when waves, currents, tsunamis, and
399 tides erode the shoreline, removing sediment and land over time. Factors such as sea-level rise,
400 wave energy, storm events, and human activities can contribute to increased rates of erosion.

401 Over time, the geomorphological landforms continue to shape and modify the landscape.
402 However, human activities and developmental pressures are significant drivers of LULC
403 change in South Andaman (Fig. 9 a, b, c). Common LULC changes observed in the area include
404 deforestation for urban expansion, conversion of land for agriculture, infrastructure
405 development, and alterations to the coastal zone (Yuvaraj et al., 2014; Thakur et al., 2017;
406 Jaman et al., 2022). The interaction between geomorphology and LULC change is particularly
407 evident in the coastal regions of South Andaman, where coastal erosion and accretion processes
408 influence both LULC patterns and development decisions. The erosion occurring near the



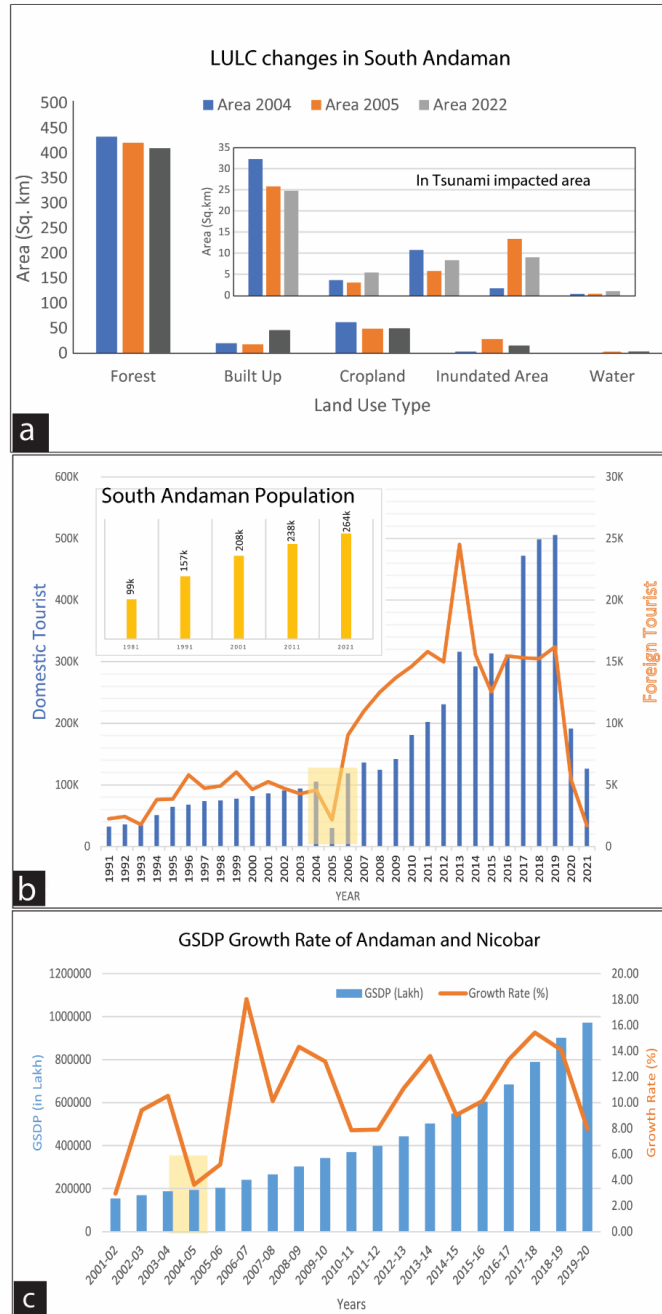
409 shoreline leads to the loss of valuable land, affecting agricultural areas, and forest regions
410 (Fig.6-8). Conversely, accretion processes can contribute to the growth of coastal areas by
411 building new landforms, and influencing land use decisions in those locations (Nagabhatla et
412 al. 2006; Ali and Narayana, 2015; Mageswaran et al. 2021).

413 **5.2 Inundation and run observation**

414 Our computations have shown that the tsunami wave heights for around 5.5 m inundation 90
415 m are observed (Fig.3 d). similarly, the harbour area of Port Blair has seen structural failures
416 in some building's foundations and our computations show wave heights of 3.6m in that area.
417 Chidiya Tapu which is 25 km from Port Blair the estimated run-up is 3.9 m and the inundation
418 is 585 m, Figure No 2 i shows a gradual slope in the region. Coming to the Southpoint Magar
419 area (Port Blair), a high run-up of 8.5 m is computed and the inundation level is 550 m. Houses
420 located near the open sea were completely washed away. At Wandoor Jetty in Port Blair, the
421 calculated runup is 3.46, the inundation is 450m, and the saltwater intrusion was observed due
422 to the tsunami.

423 **5.3 LULC vs economic change:**

424 The presence of people, infrastructure, or assets in a hazard-prone location is referred to as
425 exposure and Vulnerability is the degree to which a person, community, or system is
426 susceptible to the impacts of a hazard. Vulnerability is determined by a combination of
427 physical, social, economic, and environmental factors. (United Nations Office for Disaster Risk
428 Reduction). Several factors can contribute to changes in exposure such as population growth,
429 Industrial development, and LULC change. It is anticipated that the population of the Andaman
430 and Nicobar Islands will double by 2050 (Nanda and Haub, 2007), and the islands are
431 experiencing an increasing influx of tourists. The increased population density in these regions
432 intensifies the strain on already vulnerable lands. As a result, when a disaster, such as a natural
433 calamity, occurs in these areas, it affects the tourists and has severe repercussions for the large
434 local population heavily dependent on tourism-related activities (Annan et al., 2005; Wood et
435 al., 2019; Sathiparan et al.2020, Hamuna et al. 2019). The increases in population from 1971
436 to 2020, and built-up area is shown before and after the 2004 tsunami, and GSDP from 2001
437 to 2020 in tsunami-prone areas of South Andaman are observed in Fig. 10.



438

439 Figure 10 (a) LULC change in south Andaman and also in tsunami-affected areas of 2004. The LULC classification
 440 reveals that there has been a significant increase in built-up areas, inundated areas, and water bodies, while the
 441 agricultural land and vegetation have decreased. The increasing trends of tourists and local population in south
 442 Andaman can be seen in Fig. (b). and the GSDP growth rate shows the macroeconomic impact on GSDP in 2005
 443 due to the tsunami impact (c).



444

445 The increase in built-up areas could also positively impact the GSDP by boosting the
446 construction and real estate sectors and providing more job opportunities in the tourism and
447 hospitality industries. The 2004 Indian Ocean tsunami significantly impacted the GSDP of the
448 Andaman and Nicobar Islands, particularly in the tourism and fisheries industries. According
449 to a report by the National Institute of Disaster Management, the Andaman and Nicobar Islands
450 suffered losses amounting to INR 7.5 billion due to the 2004 tsunami, with damages to the
451 tourism industry being the most significant. It is important to carefully manage this growth and
452 ensure sustainable development practices protecting both the natural environment and the well-
453 being of the local population. This includes implementing effective disaster preparedness
454 measures, promoting sustainable tourism practices, and balancing economic development with
455 environmental conservation in the region.

456 **5.4 Implication for changing scenario of vulnerability**

457 India Inc. estimates that the total losses surpassed Rs 3,000 crore. Specifically, the losses in
458 Andaman & and Nicobar Islands exceeded Rs 1,000 crore as per industry estimates
459 (EconomicTimes.com). If a tsunami of similar magnitude were to occur again, the economic
460 loss would be five times as high as those experienced in 2004. After the 2004 tsunami, the
461 coastal area experienced significant development, with built-up areas expanding in already
462 affected areas from ~7.38 % in 2004 to ~11.11 % in 2022. This increase in urbanization and
463 infrastructure means that more properties, businesses, and critical facilities are now located in
464 the coastal zone. The affected region's local population grew from 208k people in 2001 to 264k
465 people in 2021 (Figure 10). With more people living in the coastal area, there is a higher risk
466 of casualties and a greater demand for resources and aid during and after a tsunami. The number
467 of tourists visiting the coastal area has increased significantly over the years. In 2001, there
468 were 98,000 tourists, but by 2019, this number rose to 500,000 (Figure 10). Tourists are
469 generally less familiar with local hazards and evacuation routes, making them more vulnerable
470 during a tsunami. The presence of a large number of tourists can add complexity to evacuation
471 and relief efforts, potentially leading to higher economic losses. The region has experienced a
472 sharp decline in forest and cropland areas. Forests act as natural buffers, helping to reduce the
473 impact of a tsunami by absorbing some of the wave energy. Additionally, the loss of cropland
474 can disrupt the supply chain during and after a disaster, affecting food availability and leading
475 to economic losses beyond property damage.



476 **6. Conclusions**

477 The South Andaman region is vulnerable to tsunamis due to its location in the seismically
478 active zone. In such an environment, tsunami preparedness and resilience are crucial. This
479 includes implementing effective early warning systems, raising public awareness, and
480 strengthening infrastructure resilience. Incorporating ecosystem-based approaches, such as the
481 preservation and restoration of natural coastal land, can also contribute to reducing tsunami
482 vulnerability. The South Andaman region is prone to shoreline changes due to natural processes
483 and human activities. It is crucial to monitor and assess these changes regularly to understand
484 their impacts on coastal ecosystems and communities. Implementing appropriate coastal
485 management strategies, such as beach nourishment, dune restoration, and erosion control
486 measures, can help mitigate the negative effects of shoreline changes. It is important to adopt
487 sustainable land use practices that balance economic development with the conservation and
488 responsible use of resources. This involves promoting eco-friendly tourism, protecting
489 sensitive ecosystems like mangroves and coral reefs, and implementing land use planning that
490 considers the carrying capacity and vulnerability of the region. Tsunami modeling along the
491 coastal locations shall help decision-makers how to construct structures along the coast.
492 Decision makers will also be able to quantify the tsunami impact on sloping beaches, Flat
493 beaches, and areas having boulders/mangroves. Engaging local communities, stakeholders, and
494 indigenous knowledge holders in decision-making processes and promoting capacity-building
495 initiatives are critical for ensuring the sustainable development of the Andaman region.

496

497 **Code availability**

498 No

499 **Data availability**

500 All data included in this study are available upon request by contacting the corresponding
501 author.

502 **Authors' contributions**

503 Vikas Ghadamode: Computations, Fieldwork, and Manuscript Writing.
504 K. Kumari Aruna: TUNAMI-N2 Computation and Fieldwork, Manuscript Writing
505 Anand Kumar Pandey: Manuscript Editing and Contribute Ideas and Suggestions
506 Kirti Srivastava: Paper Writing and TUNAMI-N2 Computations

507 **Competing interests / Conflicts of interest/**

508 The authors declare that they have no known conflicts of interest.

509

510 **Declarations**

511 The authors declare that they have no known conflicts of interest.

512

513



514 **Financial support**

515 No Funding

516

517 **Acknowledgements:**

518 The authors acknowledge encouragement and permission to publish from the Director, CSIR-
519 NGRI. VG acknowledges UGC, India for SRF for pursuing a PhD (Grant no.: [10/UGC-
520 JRF/209/19-ESTT](https://doi.org/10.1080/01490419.2014.908795)).

521

522 **References**

- 523 Ali, P. Y., & Narayana, A. C.: Short-term morphological and shoreline changes at Trinkat Island,
524 Andaman and Nicobar, India, after the 2004 tsunami. *Marine Geodesy*,38(1), 26-39,
525 <https://doi.org/10.1080/01490419.2014.908795> , 2015.
- 526 Annan, K.: *Reducing Risks from Tsunamis: Disaster and Development*. Nueva York: UNDP, 2005.
- 527 Bandopadhyay, P. C., & Carter, A.: Chapter 2 Introduction to the geography and geomorphology of the
528 Andaman–Nicobar Islands. *Geological Society, London, Memoirs*, 47(1), 9-18,
529 <https://doi.org/10.1144/M47.2>, 2017.
- 530 Bhat, G.R., Balaji, S. & Yousuf, M.: Tectonic geomorphology and seismic hazard of the east
531 boundary thrust in northern segment of the Sunda–Andaman subduction zone. *Nat Hazards*
532 116, 401–423, <https://doi.org/10.1007/s11069-022-05680-6>, 2023.
- 533 Boak EH, Turner IL.: Shoreline definition and detection: a review. *J Coast Res* 21:688–703,
534 <https://doi.org/10.2112/03-0071.1>, 2005.
- 535 Chen X.: Using remote sensing and GIS to analyse land cover change and its impacts on regional
536 sustainable development. *Int J Remote Sens* 23(1):107–124,
537 <https://doi.org/10.1080/01431160010007051>, 2002.
- 538 Cho, Y. S., Lakshumanan, C., Choi, B. H., & Ha, T. M.: Observations of run-up and inundation levels
539 from the teletsunami in the Andaman and Nicobar Islands: A field report. *Journal of Coastal*
540 *Research*, 24(1), 216-223, <https://doi.org/10.2112/06-0662.1>, 2008.
- 541 Cooper JA, Jackson D, Nava F, McKenna J, Malvarez G.: Storm impacts on an embayed high energy
542 coastline, western Ireland. *Marine Geol* 210:261–280,
543 <https://doi.org/10.1016/j.margeo.2004.05.012>,2004.
- 544 Curray, J. R.: Tectonics and history of the Andaman Sea region. *Journal of Asian Earth Sciences*, 25(1),
545 187-232, <https://doi.org/10.1016/j.jseae.2004.09.001>, 2005.
- 546 Davis, R.A.: Human Impact on Coasts. In: Finkl, C.W., Makowski, C. (eds) *Encyclopedia of Coastal*
547 *Science*. *Encyclopedia of Earth Sciences Series*. Springer, Cham, [https://doi.org/10.1007/978-3-
548 319-93806-6_175](https://doi.org/10.1007/978-3-319-93806-6_175), 2019.
- 549 Devi, E. U., & Sheno, S. S. C.: Tsunami and the effects on coastal morphology and ecosystems: a
550 report. *Proceedings of the Indian National Science Academy*, 78(3), 513-521,2012.



- 551 Ghosh, T., Jana, P., Giritharan, S., Bardhan, S., Basir, S. R., & Roy, A. G.:Tsunami Survey in Andaman
552 Nicobar Group of Islands. *Sumatra–Andaman Earthquake and Tsunami*, 26,2004.
- 553 Hamuna, B., Kalor, J. D., & Tablaseray, V. E.: The impact of tsunami on mangrove spatial change in
554 eastern coastal of Biak Island, Indonesia. *Journal of Ecological Engineering*, 20(3),
555 <http://dx.doi.org/10.12911/22998993/95094>, 2019.
- 556 Jaman, T., Dharanirajan, K., & Rana, S.: Land use and Land cover Change detection and Its
557 Environmental Impact on South Andaman Island, India using Kappa coefficient Statistical
558 Analysis and Geospatial Techniques, 2022.
- 559 Jangir, B., Satyanarayana, A. N. V., Swati, S., Jayaram, C., Chowdary, V. M., & Dadhwal, V. K.:
560 Delineation of spatio-temporal changes of shoreline and geomorphological features of Odisha
561 coast of India using remote sensing and GIS techniques. *Natural Hazards*, 82(3), 1437-1455,
562 <https://link.springer.com/article/10.1007/s11069-016-225>, 2016.
- 563 Jayakumar K, Malarvannan S.: Assessment of shoreline changes over the Northern Tamil Nadu Coast,
564 South India using WebGIS techniques. *J Coast Conserv.* 20(6):477–487,
565 <https://link.springer.com/article/10.1007/s11852-016-0461-9>, 2016.
- 566 Jevrejeva, S., Jackson, L., Riva, R., Grinstead, A., & Moore, J.: Sea level rise with warming above 2
567 degree. In EGU General Assembly Conference Abstracts (p. 3637), 2017.
- 568 Kumar ST, Mahendra RS, Nayak S, Radhakrishnan K, Sahu KC.: Coastal vulnerability assessment for
569 Odisha state, East coast of India. *J Coast Res* 26:523–534, <https://doi.org/10.2112/09-1186.1>,
570 2010.
- 571 Kumari P, Jnaneswari K, Rao D, Sridhar D.: Application of remote sensing and geographical
572 information system techniques on geomorphological mapping of coastal part of East Godavari
573 district. Andhra Pradesh, India. *Int J Eng Sci Tech* 4:4296–4300,
574 <https://link.springer.com/article/10.1007/s11069-016-2252>, 2012.
- 575 Mageswaran, T., Sachithanandam, V., Sridhar, R., Mahapatra, M., Purvaja, R., & Ramesh, R.: Impact
576 of sea level rise and shoreline changes in the tropical island ecosystem of Andaman and
577 Nicobar region, India. *Natural Hazards*, 109, 1717-1741,
578 <https://link.springer.com/article/10.1007/s11069-021-04895-3>, 2021.
- 579 Misra, A., & Balaji, R.: A study on the shoreline changes and Land-use/land-cover along the South
580 Gujarat coastline. *Procedia Engineering*, 116, 381-389,
581 <https://doi.org/10.1016/j.proeng.2015.08.311>, 2015.
- 582 Moran CAA.: Spatio-temporal analysis of texas shoreline changes using GIS technique. *Mediterranean*
583 *Mar Sci* 2:5–13, <https://hdl.handle.net/1969.1/408>, 2003.
- 584 Mouat DA, Lancaster J.: Use of remote sensing and GIS to identify vegetation change in the upper San
585 Pedro River watershed. *Arizona Geocarto Int* 11(2):55–67,
586 <https://doi.org/10.1080/10106049609354534>, 1996.
- 587 Mujabar S, Chandrasekhar.: A shoreline change analysis along the coast between Kanyakumari and
588 Tuticorin, India, using digital shoreline analysis system. *Geo-spatial Inf Sci* 14:282–293,
589 <https://link.springer.com/article/10.1007/s12517-011-0394-4> , 2011.



- 590 Mujabar S, Chandrasekar N.: Shoreline change analysis along the coast between Kanyakumari and
591 Tuticorin of India using remote sensing and GIS, Arab J Geosci. <https://doi.org/10.1007/s12517-011-0394-4>, 2011a.
- 593 Mujabar S, Chandrasekar N.: A Shoreline change analysis along the coast between Kanyakumari and
594 Tuticorin, India using remote sensing and GIS. Arab J Geosci 6(2013):6647–6664,
595 <https://link.springer.com/article/10.1007/s12517-011-0394-4>, 2011b.
- 596 Mukhopadhyay, A., Mukherjee, S., Hazra, S., & Mitra, D.: Sea level rise and shoreline changes: a
597 geoinformatic appraisal of Chandipur coast, Orissa. *Int J Geol Earth Environ Sci*, 1(1), 9-17,
598 2011.
- 599 Murali M, Ankitha M, Amritha S, Vethamony P.: Coastal vulnerability of Puducherry coast, India,
600 using analytical hierarchical process. *Nat Hazards Earth Syst Sci* 13:3291–3311,
601 <https://doi.org/10.5194/nhess-13-3291-2013>, 2013.
- 602 Nagabhatla, N., Roy, P. S., & Jagdale, R.: Evaluating the change (1968-2001) in landscape pattern
603 and analyzing disturbance in Baratang Forest Division (Andaman Islands), SOUTHEAST
604 ASIA, <https://hdl.handle.net/10568/40948>, 2006.
- 605 Nanda, A. R., & Haub, C.: The future population of India—a long-range demographic view. Popul Res
606 Bureau, 2007.
- 607 Natarajan, L., Sivagnanam, N., Usha, T., Chokkalingam, L., Sundar, S., Gowrappan, M., & Roy, P. D.:
608 Shoreline changes over last five decades and predictions for 2030 and 2040: a case study from
609 Cuddalore, southeast coast of India. *Earth Science Informatics*, 14(3), 1315-1325, 2021.
- 610 Nayak S.: Use of coastal data in coastal mapping. *Indian Carto CMMC* 147–156, 2002.
- 611 Prabhbir Singh., and Kamlesh Khanduri.: Land use and Land cover change detection through Remote
612 Sensing & GIS Technology: Case study of Pathankot and Dhar Kalan Tehsils. *Inter. Journal, of*
613 *Geomatics and Geosciences* 1(4), pp 839-846, 2011.
- 614 Prerna, R., Srinivasa Kumar, T., Mahendra, R. S., & Mohanty, P. C.: Assessment of Tsunami Hazard
615 Vulnerability along the coastal environs of Andaman Islands. *Natural Hazards*, 75, 701-726,
616 <https://link.springer.com/article/10.1007/s11069-014-1336-8>, 2015.
- 617 Ramalanjaona, G.: Impact of 2004 tsunami in the islands of Indian ocean: Lessons
618 learned. *Emergency Medicine International*, <https://doi.org/10.1155/2011/920813>, 2011.
- 619 Reguero, B. G., Beck, M. W., Agostini, V. N., Kramer, P., & Hancock, B., Coral reefs for coastal
620 protection: A new methodological approach and engineering case study in Grenada. *Journal of*
621 *environmental management*, 210, 146-161, <https://doi.org/10.1016/j.jenvman.2018.01.024>,
622 2018.
- 623 Reid RS, Kruska RL, Muthui N, Taye A, Wotton S, Wilson CJ.: Land-use and land-cover dynamics in
624 response to changes in climatic, biological and sociopolitical forces: the case of Southwestern
625 Ethiopia. *Landscape Ecol* 15:339–355,
626 <https://link.springer.com/article/10.1023/A:1008177712995>, 2000.



- 627 Rowland, E. D., Lolade, A. A., Nicholas, D. O., Opukumo, A. W., & Omonefe, F.: The
628 Environmental Impact of Shoreline Changes and Land Use/Land Cover Change Detection in
629 the Niger Delta Region using Geospatial Technology. *Journal of Asian Scientific Research*,
630 12(4), 237-248, 2022.
- 631 Saraf AK, Choudhary PR.: Integrated remote sensing and GIS for ground water exploration and
632 identification of artificial recharge sites. *Int J Remote Sens* 119:1825–1841,
633 <https://doi.org/10.1080/014311698215018>, 1999.
- 634 Sathiparan, N.: An assessment of building vulnerability to a tsunami in the Galle coastal area, Sri
635 Lanka. *Journal of Building Engineering*, 27, 100952,
636 <https://doi.org/10.1016/j.jobbe.2019.100952>, 2020.
- 637 Scheffers A, Scheffers S, Kelletat D.: Paleotsunami relics on the southern and central Antillean island
638 arc. *J Coast Res* 21:263–273, <https://doi.org/10.2112/03-0144.1>, 2005.
- 639 Shaw, G., & Williams, A.: Impact of the Tsunami on the Tourism Industry and Ecosystem of the
640 Andaman and Nicobar Islands, India, 2006.
- 641 Sheth, A., Sanyal, S., Jaiswal, A., & Gandhi, P.: Effects of the December 2004 Indian Ocean tsunami
642 on the Indian mainland. *Earthquake spectra*, 22(3_suppl), 435-473,
643 <https://doi.org/10.1193/1.2208562>, 2006.
- 644 Siddiqui MN, Maajid S.: Monitoring of geo-morphological changes for planning reclamation work in
645 coastal area of Karachi, Pakistan. *Adv Space Res* 33:1200–1205,
646 [https://doi.org/10.1016/S0273-1177\(03\)00373-9](https://doi.org/10.1016/S0273-1177(03)00373-9), 2004.
- 647 Siva M.: Behera MR. Effect of continental slope on N-wave type tsunami run-up. *The International*
648 *Journal of Ocean and Climate Systems*, <https://doi.org/10.1177/1759313116656865>, 2016.
- 649 South Andaman District – Population.: [https://www.census2011.co.in/census/district/53-south-](https://www.census2011.co.in/census/district/53-south-andaman.html)
650 [andaman.html](https://www.census2011.co.in/census/district/53-south-andaman.html), 2011-2023.
- 651 Sudha Rani NNV, Satyanarayana ANV, Bhaskaran PK.: Coastal vulnerability assessment studies over
652 India: a review. *Nat Hazards*, <https://link.springer.com/article/10.1007/s11069-015-1597->
653 2015.
- 654 Thakur, S., Dharanirajan, K., Ghosh, P. B., Das, P., & De, T. K.: Influence of anthropogenic
655 activities on the land use pattern of South Andaman Islands. *Research Journal of Marine*
656 *Sciences*, 5(1), 1-10, 2017.
- 657 The Economic Times: [https://economictimes.indiatimes.com/tsunami-hits-india-inc-with-rs-](https://economictimes.indiatimes.com/tsunami-hits-india-inc-with-rs-3000-cr-loss/articleshow/974281.cms?from=mdr)
658 [3000-cr-loss/articleshow/974281.cms?from=mdr](https://economictimes.indiatimes.com/tsunami-hits-india-inc-with-rs-3000-cr-loss/articleshow/974281.cms?from=mdr)
- 659 Thielier ER, Himmelstoss EA, Zichichi JL, Ergul A.: Digital shoreline analysis system (DSAS)
660 version 4.0-an ArcGIS extension for calculating shoreline change. U.S. Geological Survey
661 open-file report 2008–1278. U.S. Geological Survey, Woods Hole,
662 <https://doi.org/10.3133/ofr20081278>, 2009.
- 663 Tonisso H, Suursarr U, Kont A.: Maps, aerial photographs, orthophotos and GPS data as a source of
664 information to determine shoreline changes, coastal geomorphic processes and their relation to



- 665 hydrodynamic conditions on Osmussa island, The Baltic sea. *IGRSS* 12:987–1159,
666 <https://doi.org/10.1109/IGARSS.2012.6350382>, 2012.
- 667 Velmurugan, A., Swarnam, T. P., & Ravisankar, N.: Assessment of tsunami impact in South
668 Andaman using remote sensing and GIS. *J. Indian Soc. Remote Sensing*, 34(2), 193-202, 2006.
- 669 Weng Q.: Land use change analysis in the Zhujiang Delta of China using satellite remote sensing, GIS,
670 and stochastic modeling. *J Environ Manag* 64:273–28,
671 <https://doi.org/10.1006/jema.2001.0509>, 2002.
- 672 Wood, N., Jones, J. M., Yamazaki, Y., Cheung, K. F., Brown, J., Jones, J. L., & Abdollahian, N.:
673 Population vulnerability to tsunami hazards informed by previous and projected disasters: a
674 case study of American Samoa. *Natural Hazards*, 95, 505-528,
675 <https://link.springer.com/article/10.1007/s11069-018-3493-7>, 2019.
- 676 Yunus, A. P., & Narayana, A. C.: Short-term morphological and shoreline changes at Trinkat Island,
677 Andaman and Nicobar, India, after the 2004 tsunami. *Marine Geodesy*, 38(1), 26-39,
678 <https://doi.org/10.1080/01490419.2014.908795>, 2015.
- 679 Yunus, A. P., Dou, J., Avtar, R., & Narayana, A.: Shoreline and coastal morphological changes induced
680 by the 2004 Indian Ocean tsunami in the Katchal Island, Andaman and Nicobar—a study using
681 archived satellite images. In *Tsunamis and earthquakes in coastal environments* (pp. 65-77).
682 Springer, Cham, https://link.springer.com/chapter/10.1007/978-3-319-28528-3_5, 2016.
- 683 Yuvaraj, E., Saravanan, E., & Dharanirajan, K.: Assessment of land use and land cover changes in south
684 Andaman Island using remote sensing and GIS. *Int J Geomat Geosci*, 5, 171-181, 2014.
- 685 Yi, L., Chen, J., Jin, Z., Quan, Y., Han, P., Guan, S., & Jiang, X.: Impacts of human activities on
686 coastal ecological environment during the rapid urbanization process in Shenzhen, China.
687 *Ocean & coastal management*, 154, 121-132,
688 <https://doi.org/10.1016/j.ocecoaman.2018.01.005>, 2018.